EES Catalysis

PAPER

View Article Online
View Journal | View Issue

Cite this: *EES Catal.*, 2025, 3, 1327

Techno-economic analysis of plasma-assisted CO_2 hydrogenation to methanol: feasibility and the impact of electricity supply

Giulia De Felice, Simona Eichkorn, Fausto Gallucci and Sirui Li *

CO_2 hydrogenation to methanol using plasma provides a sustainable alternative to conventional, fossil-based production methods. Although numerous experimental studies in relevant field have been reported, a comprehensive techno-economic assessment is still lacking. Additionally, the influence of electricity supply strategies on the plasma process remains unexplored. Therefore, in this study, evaluation has been performed on a plasma-assisted methanol production process with emphasis on the effects of multiple electricity supply strategies. A process model was developed based on the state-of-the-art performance of a catalytic DBD plasma reactor. Then, the minimum methanol selling price (MMSP) was calculated to evaluate the economic feasibility of variable and continuous operation of the plasma process and different electricity supply strategies. The results indicated that, in all scenarios investigated, the plasma process can not directly compete with conventional benchmark processes. Among the prospective power supply strategies projected for 2050, a significant reduction in MMSP was observed, with the lowest MMSP achieved when using surplus renewable energy. However, even with this approach, the MMSP was 7277 € per t, more than seven times higher than the benchmark price. Continuous operation of the plasma process at maximum capacity could improve its economic performance enabling a reduction of the MMSP to 3601 € per t.

Received 28th April 2025,
Accepted 5th August 2025

DOI: 10.1039/d5ey00130g

rsc.li/eescatalysis

Broader context

The paper presents a novel technoeconomic assessment of plasma-based methanol production, emphasizing the critical role of electricity supply in shaping the process's feasibility. Unlike conventional studies on methanol synthesis, this work proposes a plasma-based system integrated in a full scale chemical plant. It innovatively links the performance of plasma reactors with variable renewable electricity, exploring scenarios such as grid-connected systems, dedicated renewable setups, and hybrid configurations. The study highlights how the choice of electricity supply significantly impacts methanol production costs and overall system viability. Among the prospective power supply strategies projected for 2050, a significant reduction in MMSP was observed, with the lowest MMSP achieved when using surplus renewable energy. However, the results indicated that, in all scenarios investigated, the plasma process cannot directly compete with conventional benchmark processes. Still, this comprehensive approach, combining engineering design with economic analysis, provides insights into how plasma methanol production can align with renewable energy systems to support decarbonization goals.

1. Introduction

The energy transition, essential for achieving sustainable development, is already underway as we shift from fossil fuel dependence toward renewable energy sources. In the year 2022, renewable electricity generated from wind and solar reached 11.7% of the global electricity mix with a growth of 18.2% from 2021.[1] This significant growth helped prevent around 465 Mt CO_2 being emitted into the atmosphere.[2,3] However, as we move away from fossil fuels, efficient storage solutions are essential to harness the increased share of intermittent renewable energy.[4] At present, the available storage capacity is still limited, compared with power generation capacity.[5] A potential solution is to convert the surplus sustainable electricity into chemical energy.[6,7] Power-to-X technologies, which facilitate the conversion of electricity into various energy carriers, are essential for enhancing energy flexibility and supporting decarbonization efforts.[8] Additionally, converting GHGs into chemicals not only provides a viable and sustainable energy storage solution but also contributes to emission mitigation, further supporting environmental goals.[9]

CO_2 valorisation has attracted considerable attention in recent years, with various processes explored. In these

Department of Chemical Engineering and Chemistry, Eindhoven University of Technology, Eindhoven 5612 AZ, The Netherlands. E-mail: s.li@tue.nl

approaches, CO_2 serves as a reactant to produce high-value products such as methanol, methane, and longer-chain hydrocarbons, thereby contributing to both emission reduction and resource recovery.[10,11] Among the possible products, methanol is particularly promising as it can be used as a fuel in internal combustion engines and fuel cells. It has high energy density and is easy to transport and store.[12] Furthermore, with advanced zeolite-based catalysts, methanol can be converted into essential chemicals such as olefins (*via* methanol-to-olefins, MTO).[13] The versatile applications led to growth of the methanol market, which is expected to continue in the coming years, with forecasts projecting it to exceed 135 million tons by 2030.[14]

Thermodynamically the production of methanol is favoured at low temperature; however in thermal catalysis, elevated temperatures are required to activate the CO_2 molecule. Besides, the high temperature also promotes the reverse water gas shift reaction to produce CO, which is the main reaction competing with the methanol production.[15,16] As an alternative to conventional methods, activating CO_2 through non-thermal plasma (NTP) presents a promising and emerging approach. The combination of plasma with catalysts, known as plasma-catalysis, has great potential for methanol production in a more sustainable and energy-efficient way, bypassing the high energy requirements typically associated with traditional catalytic processes.[17] Many studies on CO_2 hydrogenation have been conducted to investigate plasma-catalytic methanol production.

Table 1 shows examples of results reported in the literature, including the CO_2 conversion, CH_3OH yield, and the energy consumption achieved. Within these studies different catalysts and conditions were investigated.

Methanol production *via* non NTP processes has been demonstrated on a laboratory scale with interesting results in terms of conversion and energy consumption; however the economic feasibility of this process at an industrial scale has not yet been researched. A comprehensive understanding at the process level is currently lacking, which limits the optimization and scalability of non-thermal plasma-based CO_2 conversion for methanol production. To address these gaps, a techno-economic assessment (TEA) is essential, as it would provide a structured evaluation of costs, benefits, and potential economic impacts at an early stage of development. Furthermore, a major advantage of plasma processes is their ease of integration with intermittent renewable electricity, a benefit frequently noted in relevant publications.[24] However, understanding this integration remains limited, and the impact of various electricity supply strategies on plasma process performance is still unknown.

Therefore, this study provides a prospective analysis centred on evaluating the impact of electricity supply strategies on the techno-economic feasibility of methanol synthesis *via* CO_2 hydrogenation. In this work, different sources including electricity drawn from the main grid, surplus electricity generated from renewable sources (such as excess solar or wind power that might otherwise go unused), and on-site electricity produced by a dedicated wind turbine and solar panels is investigated. The main goal is to identify the main cost drivers of the different configurations, as well as guidelines on how to further develop these systems towards future industrial applications.

Table 1 Overview of plasma-assisted methanol synthesis processes

Catalyst	CO_2 conversion	CH_3OH yield	Energy consumption	Ref.
[—]	[%]	[%]	[kJ $mmol_{CH_3OH}^{-1}$]	[—]
Cu/Al_2O_3	10	4.75	41.6	18
Cu/Al_2O_3	21.3	11.3	11.9	19
$Pt/film/In_2O_3$	37	23.16	—	20
CuO/Fe_2O_3/QW	16	5.23	—	21
CuO–MgO/beta	8.5	6.12	17.9	22
Fe_2O_3/Al_2O_3	12	7.04	19.8	23

2. General methodology and process design assumptions

In this assessment, alternative electricity supply configurations were analyzed to determine their economic feasibility and impact on methanol production costs. Specifically, two processes were compared: (1) a continuous process powered by electricity from the grid, or a mix of grid and surplus electricity, and (2) a partially continuous process supplied by surplus electricity only, or electricity generated from wind turbines or solar panels. Both processes are designed for a scale comparable to existing ozone production plants, a typical industrial plasma process utilizing DBD reactors, enabling a realistic assessment of the system's economic and operational performance. Indeed, although gliding arc (GA) and microwave (MW) plasmas achieve higher temperatures and greater efficiency for CO_2 conversion, DBD reactors offer several practical advantages. They are scalable and allow easier sustainment of stable non-thermal plasma. Additionally, they have simpler designs and require less maintenance compared to GA. Furthermore, CO_2 hydrogenation to methanol is an exothermic reaction, and the lower operating temperatures of DBD reactors are more favourable for methanol production.[25] Currently large scale industrial DBD systems operate in the MW range.[26] In this case, a target capacity of 195 MW was selected based on the highest power investigated by Kaufmann *et al.*[27] Furthermore, we assume a plant lifetime of 20 years, with a production time of 8760 h. To understand the economic feasibility of each configuration, the analysis was made with a focus on the impact of capital investment (CAPEX) and operational expenses (OPEX) on the minimum methanol selling price (MMSP) required.

2.1 System boundaries

This study focuses on methanol production while the CO_2 capture, purification, and transport, as well as the H_2 generation and transport are not considered in the process. As a base case, we assumed that CO_2 is obtained *via* the sorption enhanced water gas shift (SEWGS) process from iron and steel off-gases,[28] while H_2 is assumed to be supplied by an integrated pipeline network. The H_2 and CO_2 streams are assumed to enter the plant at 30 °C (303 K) and atmospheric pressure.

The purities of both streams are 100% since the purification generally takes place at the site of generation.

The determination of the plant location was based on several factors, such as resource availability, construction and operating costs and the product market. At present, there is a discrepancy between supply and demand within Europe. As a result, this offset of methanol demand needs to be imported to Europe. Within the EU the ''Industrial Emissions Directive'' holds, which regulates the levels of pollution which industries can cause. In order to comply with this to the full extend, it is beneficial to use locally produced chemicals, rather than to use imports from countries with different emission standards. As a result, methanol production in Europe is a relevant scenario to investigate. Within Europe the plant location for this project was chosen to be in the Netherlands. The Netherlands is currently working on the implementation of an extensive national hydrogen pipeline network, making it a suitable candidate due to ease of future resource availability.[29] Additionally, the Netherlands has a significant chemical industry in place making local production of methanol relevant, as well as obtaining captured CO_2 feasible.

2.2 Basis and assumptions for process modelling

Mass and energy balance calculations were conducted *via* process flow modelling using Aspen Plus V11 software. The thermodynamic property method NRTL-RK was chosen for the simulation, as suggested by previous studies on CO_2 hydrogenation and decision tree.[30–32] For the refrigeration cycle using propylene the property method REFPROP is used, which is commonly applied when simulating refrigeration.[33]

The simulation of the dielectric barrier reactor for methanol production is performed according to experimental results on the conversion of CO_2 and the selectivity of the products. In Aspen Plus the reactor was modelled as a stoichiometric reactor. More specifically, the research of Wang *et al.* was found to have relatively high conversion of CO_2, high selectivity to methanol and the lowest reported energy consumption.[19] Additionally, the study provided a complete set of data, reported in Table 1, including details on the experimental set-up and parameters, conversion of CO_2 and selectivity of all obtained products. As a result, this paper was deemed suitable to provide the data for the simulation of the plasma reactors. Furthermore, to investigate the scenario of improved system performance, a case of higher methanol yield was considered, to determine the effects on the economics of the process. A study by Men *et al.* was able to achieve a yield of approximately 23%, the best reported value to our knowledge, therefore it is used as the benchmark for the high yield scenario.[20] Since no data on energy consumption were available in this case, the energy consumption data from Wang *et al.*[19] were employed to simulate the complete high-yield case.

The scale up of the plasma reactors is conducted *via* a combination of numbering up and sizing up approaches to reach the desired industrial flow. Currently, commercial processes for ozone generation employ tubular DBD reactors with 1–3 m length and 2–5 cm diameter to reach the required throughput capacities.[34–37] Thus, the DBD reactors in this study are assumed to have an inner diameter of 5 cm, with a HV electrode of 5 mm diameter and a discharge length of 3 m. In the SI, the number of reactors and the number of reactor bundles required are reported. A reactor refers to a single DBD tube, while a reactor bundle is 400 DBD tubes in parallel.

The space time, as defined in eqn (1), is fixed to 3.18 s be the same as the reported value by Wang *et al.*[19] The required flow rate per DBD tube can be calculated accordingly, as reported in the SI. It was assumed that the scaled-up reactor would achieve the same performance in terms of CO_2 conversion and methanol selectivity under identical space time conditions. This assumption is in line with the study of Assadi *et al.*, where the authors tested lab and pilot reactor scales for VOC removal keeping the same space time. In the study, the feasibility of the scale-up process by this assumption was demonstrated due to continuity of the experimental results obtained.[38]

$$\text{Space time [s]} = \frac{V_{\text{empty reactor}}\ [\text{mL}]}{Q_{\text{reactor}}\ [\text{mL min}^{-1}]} \cdot 60\ [\text{s min}^{-1}] \quad (1)$$

Additionally, the effect of the scale up on energy efficiency and power consumption needs to be considered. The specific energy input (SEI) is an important factor influencing the reactor performance.[39,40] Within the present work, this parameter is fixed to 15 000 kJ m^{-3}. Consequently, the plasma power scales linearly with volumetric flow rate, as can be seen in eqn (2). Keeping both the space time and the SEI fixed causes the methanol production and the plasma power to scale linearly with the inflow. This results in the theoretical energy consumption (eqn (3)) of the plasma system being fixed as well during scale up, assuming constant methanol yield.

$$\text{SEI}\ [\text{kJ L}^{-1}] = \frac{\text{Plasma power [W]}}{Q_{\text{total}}\ [\text{mL min}^{-1}]} \cdot 60\ [\text{s min}^{-1}] \quad (2)$$

$$\text{Energy consumption}\ [\text{J mol}^{-1}] = \frac{\text{Plasma power [W]}}{\text{Methanol produced [mol h}^{-1}]} \cdot 3660\ [\text{s h}^{-1}] \quad (3)$$

Regarding the separation section, the gas liquid separators design was based on sensitivity analyses to determine the temperature and pressure necessary to achieve a 90% recovery of methanol in the liquid phase. The distillation columns design and optimization were conducted using the DTSW and RadFrac models in Aspen Plus. The number of stages (N), reflux ratio (R), feed position and the distillate-to-feed ratio (D/F) were first estimated *via* the DSTW and later optimized by means of a more rigorous model (RadFrac), which allows the mass and energy balance of the system to be determined. A Murphee efficiency of 85% to account for deviation from the equilibrium was assumed. Column internals are trayed and the column diameter, tray spacing and hole area/active area ratio were optimized to avoid drying up and with an 80% approach to flooding.

All the turbomachines (compressors, pumps, and steam turbines) were modelled in Aspen Plus assuming an isentropic and a mechanical efficiency to determine the thermodynamic

conditions of the outlet stream and the energy balance. The isentropic and mechanical efficiency was assumed to be 0.85 and 0.95 for compressors and pumps, respectively.[41]

2.3 Basis and assumptions for cost assessment

The capital cost estimation (CAPEX) and the operating cost estimation (OPEX) were calculated based on correlations described by Seider *et al.*[42] The costs calculated were adjusted to the year 2023 using the chemical engineering plant cost index (CEPCI).[43] The operating cost estimates were adjusted using the U.S. Bureau of Labor Statistics' standard producer price index (PPI) for chemical manufacturing.[44,45] The main outcome of this economic analysis was the minimum selling price of methanol for the different scenarios, which was calculated based on a net present value (NPV) of zero.

To estimate the cost of the plasma system, a cost correlation from a study by Kaufmann *et al.* was used.[27] Herein the cost of the reactor system was calculated as a function of the power in kW, as can be seen in eqn (4).

$$\text{DBD reactor cost [Mio EUR]} = 0.05614 P_{\text{DBD}}\,[\text{kW}]^{0.5331} \quad (4)$$

It is important to note that the reactor cost includes the cost of the power supply unit. P_{DBD} refers to the power input to the power supply unit, meaning the efficiency of the power supply needs to be considered. Based on the literature reviewed, it is estimated that approximately 50% of the P_{DBD} can be employed for the reactor to carry out the reaction.[46] Furthermore, the calculated cost of the reactor includes the reactors themselves as well as the power supply. The power supply was expected to be the largest contribution to the capital cost of the overall plasma system. This dominant contribution of the power supply was also found in similar studies by Van Rooij *et al.* and Van Assche *et al.*[46,47]

The catalyst used within the plasma-catalytic system is Cu/γ-Al_2O_3. This catalyst is currently not commercially available, making it difficult to obtain the bulk price. In order to get an estimation of the cost the approach published by Baddour *et al.* on a step-based method for the price estimation for precommercial heterogeneous catalysts is used.[48] Firstly, the price estimation method requires detailed information on the catalyst synthesis, including the inputs used in the laboratory-scale procedure. The synthesis steps described by Wang *et al.* provide the basis for translating the lab procedure into industrially relevant process steps. These steps include, for example, incipient wetness impregnation and drying in a rotary dryer (at 100–300 °C). Secondly, the method requires defining the market or application in which the catalyst will be used (business inputs). This enables the assignment of appropriate hourly costs for process equipment typically used in commercial catalyst production. The Baddour method supports this process by providing a table of typical production steps along with their corresponding estimated costs at different production scales (small, medium, large). This method relies on distinct processing steps; each linked to specific process equipment utilized by a contract catalyst manufacturer. It accounts for all capital and operating costs, including equipment acquisition, maintenance, labour, and utilities.

Table 2 Total capital investment calculation using Lang factors[42]

	Lang factor
Delivered cost of process equipment	1
Installation	0.47
Instrumentation and control	0.36
Piping	0.68
Electrical	0.11
Buildings (including services)	0.18
Yard improvements	0.1
Service facilities	0.7
Total direct plant cost	**3.6**
Engineering and supervision	0.33
Construction expenses	0.41
Total direct and indirect plant costs	**4.34**
Contractor's fee and legal expenses	0.26
Contingency	0.44
Fixed capital investment	**5.04**
Working capital	0.89
Total capital investment	**5.93**

To calculate the required capital investment for the designed solar and wind systems, a study by Sens *et al.* is applied.[49] Herein, the learning rates for the period between 2012 and 2020 are used to calculate predictions for the capital investment of these systems in 2030 and 2050. The capital investments are predicted as a factor of the installed capacity as € per kW. The prediction for the solar system is 235 € per kW and for the wind system 966 € per kW.

In order to estimate the total capital investment needed for this project the overall factor method of Lang was used, which is detailed in ref. 42. Table 2 shows a summary of the Lang factors (f_L) used to estimate the total capital investment.

The variable operating costs include the cost of the feedstock (*i.e.*, CO_2 and H_2), utilities (*i.e.*, electricity), the wastewater treatment and the cost for the catalyst, for which a lifetime of 1 year is assumed. The CEPCI factors are used to adjust the operating costs to the current year, to account of developments in prices over time. On the other hand, the fixed operating costs consist of labour costs, maintenance costs, overhead, taxes and general expenses. 20 operators were assumed, following the procedure described in ref. 42. A detailed outline of the methodology used to calculate these costs can be seen in Table 3.

In order to account for the costs from the capital investment, the annualized capital costs were calculated, according to the methodology reported in the SI. The minimum methanol selling price (MMSP) was determined by calculating the required price to obtain a net present value (NPV) of zero, and the procedure is reported in the SI. A debt/equity ratio of 50/50 is assumed. The debt interest rate (r_d) is 3.5%, and a cost of equity (r_e) of 12%.[51,52] The plant lifetime is expected to be 20 years. During the first two years, only partial production is assumed, resulting in 30% and 70% of the revenue and annual costs. The startup costs are estimated as 10% of the total depreciable capital, which is the capital cost without the working capital.[42]

Table 3 Overview of the method used to calculate the fixed operating costs[42]

Operations (O)	
Direct wages and benefits (DW&B)	60 000 € per operator-year[50]
Direct salaries and benefits	15% of DW&B
Operating supplies and services	6% of DW&B
Maintenance (M)	
Wages and benefits (MW&B)	3.5% of C_{TDC}
Salaries and benefits	25% of MW&B
Materials and services	100% of MW&B
Maintenance overhead	5% of MW&B
Operating overhead	
General plant overhead	7.1% of M&O–SW&B
Mechanical department services	2.4% of M&O–SW&B
Employee relations department	5.9% of M&O–SW&B
Business services	7.4% of M&O–SW&B
Property taxes and insurance	2% of C_{TDC}
Cost of manufacturing (COM)	**Sum of the above**
General expenses	
Selling expenses	3% of sales revenue
Direct research	4.8% of sales revenue
Allocated research	0.5% of sales revenue
Administrative expenses	2% of sales revenue
Management incentive compensation	1.25% of sales revenue
Total general expenses (GE)	**Sum of the above**
Total production cost	**COM + GE**

A depreciation period of 10 years is assumed, with a salvage value of zero and straight line depreciation.[51] The exchange rate used is 1 USD to 0.92 €.[53]

3. Process design

3.1 Plasma assisted CO_2 hydrogenation plant

The upscaled process of plasma-assisted methanol production uses multiple DBD reactors in parallel to achieve the desired throughput. 2.46 kt_{CH_3OH} per year and 5.01 kt_{CH_3OH} per year at low methanol yield and high methanol yield were obtained, respectively. After which, a separation train follows to obtain methanol at its desired purity. The process flow diagram (PFD) of this system can be seen in Fig. 1. The outflow of the reactors is a gas and liquid mixture containing unreacted CO_2 and H_2 together with methanol and byproducts. Initially the gaseous components CO_2, H_2, CO and CH_4 are separated in a cryogenic separator at −20.5 °C, obtaining also a liquid stream composed of mainly CH_3OH, C_2H_5OH and H_2O. At this temperature 90% of the methanol product is recovered in the liquid stream. The separated gaseous stream is then recycled, after having a purge stream of 5% to minimize inert byproduct buildup. This section of the system can be operated both at variable load as well as at steady state. Afterwards, the crude methanol is purified in a stripping column using H_2 as the stripping gas to remove dissolved CO_2. This method was suggested in a study by Kiss *et al.*, where high pressure H_2 was used to strip CO_2.[54] For the purpose of integration with the plasma process, the stripping column is designed at atmospheric pressure, as all streams are at low pressure. The hydrogen flow is set based on the CO_2 removal, the CH_3OH loss (below 1%) and the hydraulics of the column, ensuring that the operating point of the column falls within the operating region, where no flooding or weeping is observed. After this step two distillation columns are required. The first distillation column removes water as the bottom product and the second distillation column separates the ethanol contained in the mixture at the bottom. As a first indication the two distillation columns were designed using the shortcut DSTWU column, by setting the reflux ratio to $1.2R_{min}$. Hereby an initial reflux ratio and number of stages is determined. To obtain a more robust design these specifications are then used in the design of a RadFrac column. Herein the number of stages, the reflux ratio and the distillate to feed ratio are supplied. A Murphree efficiency of 85% is assumed, to reflect any deviation from equilibrium.[55] To obtain the desired recoveries, two design specifications (DSs) are used. The first DS sets the molar methanol recovery to 99% by adjusting the distillate to feed ratio. The second DS adjusts the reflux ratio to obtain a water recovery on the top of 2%, ensuring 98% of the water goes to the bottom section. In the second column a partial condenser is used to obtain a vapour distillate including light components and a liquid distillate which is the final purified methanol stream. A final required mass purity of 99.85 wt% methanol is obtained. In this column, a partial condenser with a condenser temperature of 39 °C is used. The feed stage is optimized by investigating the composition profile across the columns and ensuring a smooth composition change throughout the column, avoiding significant jumps at any stage. The number of stages was adjusted as a final step, to a point where the reflux ratio no longer decreases significantly to warrant additional stages. The column internals, such as the column diameter, tray spacing and hole area/active area ratio were optimized for sieve trays to ensure operation within the operating region. Hereby possible flooding, weeping or drying up during operation is avoided.

Within this process there are two types of units, ones that can be operated variably and ones that need to be operated in continuous operation. For instance, DBD reactors have the ability to operate at variable input. Gas liquid separators are equilibrium units which can operate at partial load as long as the design capacity is not exceeded. In contrast, the stripper and the distillation columns are units that need to be operated continuously at steady-state. Therefore, the overall system can either be run fully continuous or it can be run partially continuous. When the plasma system is operated continuously at a certain capacity by providing a constant supply of electricity, the crude methanol from the plasma system can be directly purified in the separation train.

Alternatively, the process can be operated partially continuous (Fig. 2). In the case of direct renewable energy supply, the amount of electricity available varies, meaning the production capacity of the plasma reactors and the throughput of the initial gas liquid separation is at variable load. After this gas liquid separation, an intermediate storage tank is installed

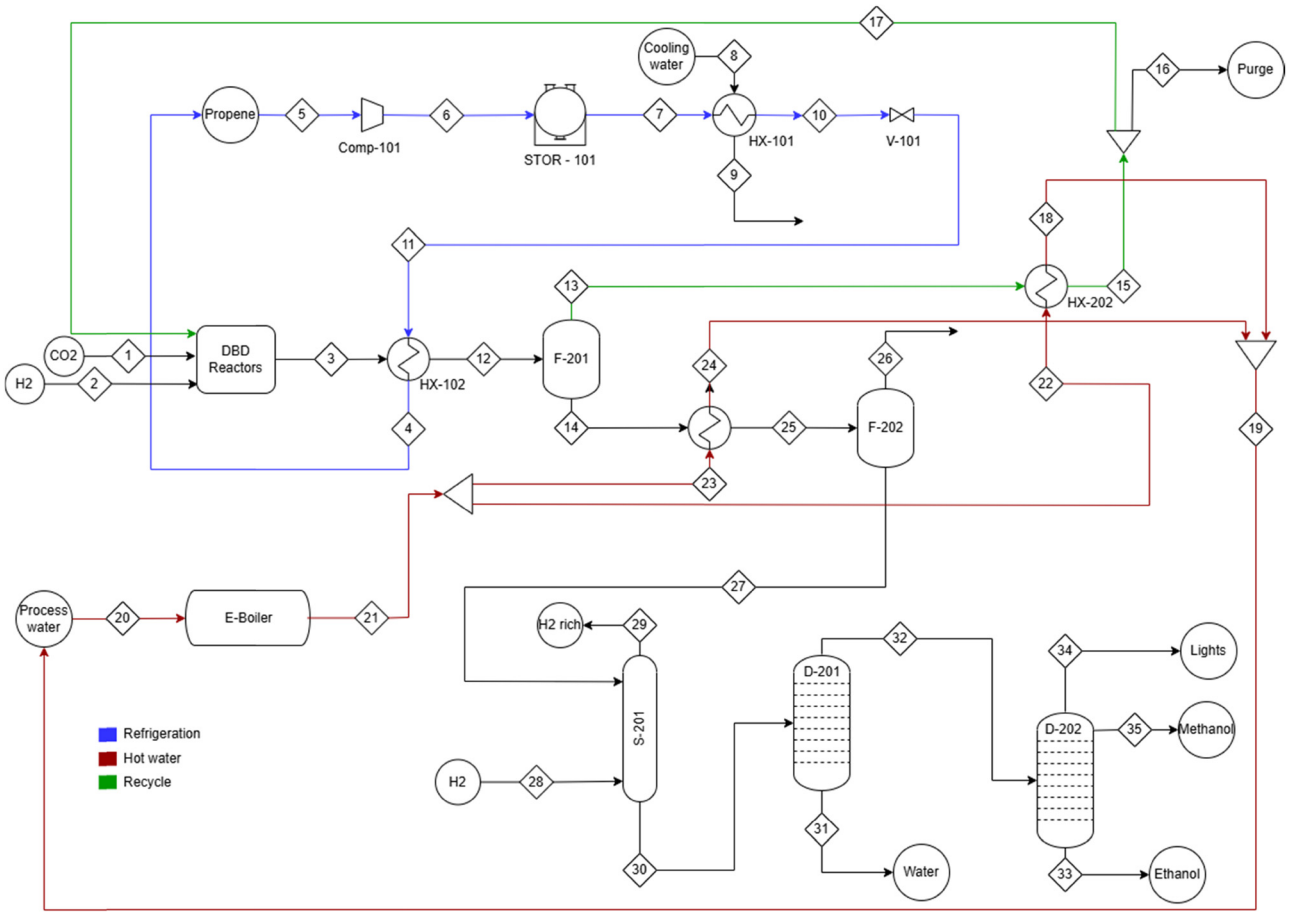

Fig. 1 PFD showing a fully continuous system.

which ensures a constant steady supply of crude methanol to the stripping and distillation section. The outflow of the storage tank, in mol h^{-1}, is set to the yearly average flow of crude methanol. In order to ensure that the storage tank does not run dry, it initially needs to be filled to a certain level. To determine the required initial load of crude methanol, a mass balance across the storage tank was set up. As a safety margin, it was implemented that the storage tank does not empty below 10% of the maximum filling. Using a solver, the required initial filling was determined by ensuring the accumulation is maintained above 10% of the maximum filling. Based on this and the density of the mixture obtained from Aspen Plus, the required volume of the storage tank could be determined. Hence, the production section of the system can operate variably while the downstream separation operates at steady state.

3.2 Technical comparison

In this study, five different scenarios are discussed, as listed in Table 4. For each scenario two sub-scenarios are identified, namely a "low-yield case" based on the yield and energy consumption by Wang *et al.*[19] and a "high-yield case" based on the yield reported by Men *et al.*,[20] both reported in Table 1.

- Scenario #1

A study by TNO, conducted by Sijm *et al.*, investigated the prospective power system of the Netherlands.[56] This study uses the COMPETES model (competition and market power in electric transmission and energy simulator) to predict the power generation and utilization at an hourly resolution. In the study, four methods of flexible demand response were included, namely power to H_2, power to heat (industry), power to heat (household) and power to mobility (electric vehicles). With these mentioned factors, the demand is optimized, however there is still a significant amount of electricity that needs to be curtailed to avoid overloading the grid. The electricity that needs to be curtailed is viewed as excess renewable energy that could be utilized for plasma-assisted methanol production. The TNO study predicts a price of 0.002 € per kWh for the curtailed electricity.[56]

Taking into account the curtailed electricity profile which is shown in Fig. 3a, the size of the plasma system has been established. The design power of the plasma system and the electricity available directly determines the amount of methanol that is produced. The chosen design power corresponds to the maximum capacity at which the plasma system can operate at. If there is less power available, the system operates at a reduced capacity, adjusted to the electricity availability. When more electricity is at hand the system operates at its maximum capacity.

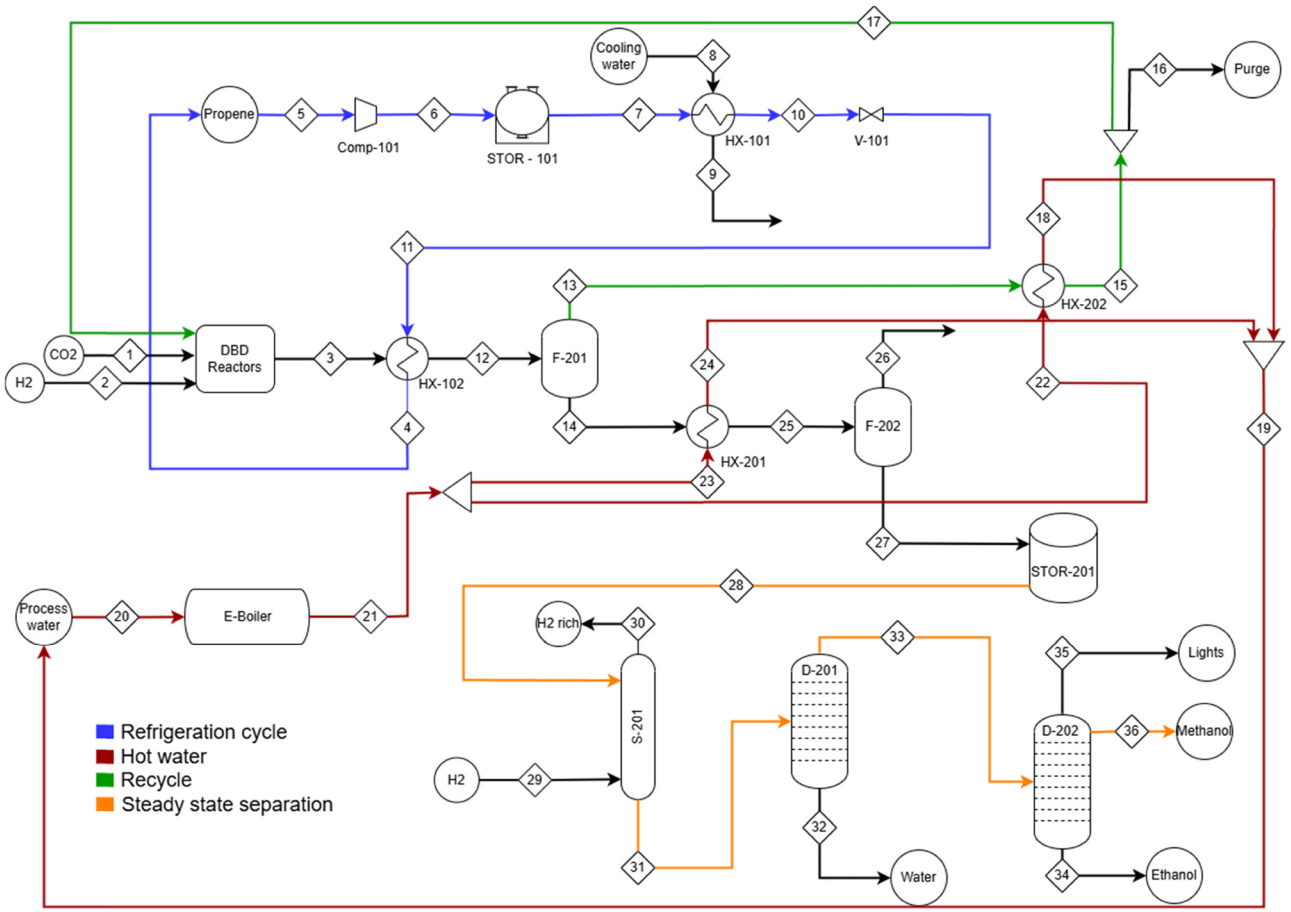

Fig. 2 PFD showing a partially continuous system with intermediate storage of crude methanol.

Table 4 Overview of the scenarios analyzed in this study

	Scenario	Features	Year
#1	Surplus electricity	The plant is powered with surplus electricity from renewable energy sources.	2050
#2	Wind power	The plant is powered with electricity from an off-grid wind system.	2050
#3	Solar power	The plant is powered with electricity from an off-grid solar system.	2050
#4	Continuous electricity	The plant is powered with electricity supplied from the grid.	2023
#5	Surplus & grid	The plant is powered with a combination of surplus electricity and electricity supplied from the grid.	2050

Using the surplus electricity data for 2050, the total power available for methanol production has been determined. This was done by summing the system power over the full year, resulting in a total power consumption of 508.42 GWh per year. As a result, the production capacity at low methanol yield of 2.46 kt_{CH_3OH} per year can be obtained, and 5.01 kt_{CH_3OH} per year at the high methanol yield. The mass balances are reported in Tables S1 and S2 in the SI. This production capacity was kept constant for scenario #2, scenario #3 and scenario #4, to ensure direct comparability.

- Scenario #2

In scenario #2, an off-grid solar system was designed in the Netherlands, such that the solar system can supply the same amount of power to the plasma system (508.42 GWh per year). Due to the variable availability and intensity of sunlight the system is not used at the same capacity throughout the year (Fig. 3b). Therefore, predictions are needed on the amount of solar energy produced yearly, to determine the required size of the solar system. The aforementioned TNO report on the power system in the Netherlands provided predictions for the capacity factor (CF) of solar power systems in the Netherlands for the year 2050 (eqn (5)).

$$\text{CF}\ [-] = \frac{\text{Actual electrical energy input [W]}}{\text{Maximum capacity of the system [W]}} \quad (5)$$

These calculations result in a solar system with a required capacity of 810.4 MW, to provide the total required power to the plasma system on a yearly basis. The capacity of the solar system is significantly above the power of the plasma system, as the CFs for solar production are relatively low and also

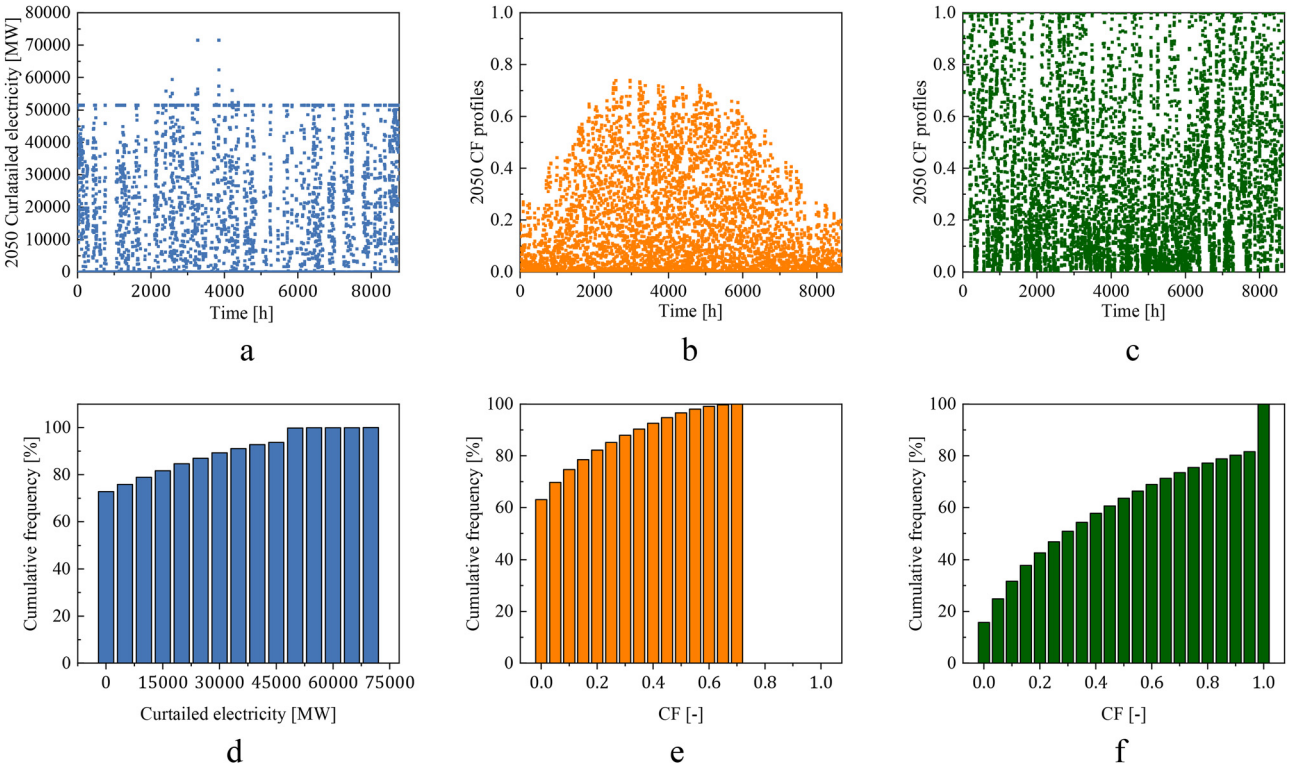

Fig. 3 Predicted hourly profile and cumulative frequency of (a) and (d) curtailed electricity including demand response in 2050, (b) and (e) capacity factor for solar energy in 2050 and (c) and (f) capacity factor for wind energy in 2050, data plotted from ref. 56, with permission from the author in TNO.

strongly variable throughout the year. Due to this large capacity, there will be periods where more than 195 MW of power is produced. This will result in an excess of electricity which can be sold and provide an additional source of income. The size of the solar park falls in a feasible range and similar solar parks have been realized in China, India and UAE. At present, the largest solar farm in the world is located in China with a capacity of 2.8 GW.[57] In Europe the largest solar farm started operating in March 2024 in Germany, with a capacity of 605 MW.[58]

• Scenario #3

In scenario #3, an off-grid system based on wind energy is designed. In principle the same methodology is applied as for scenario #2. The total power provided to the plasma is 508.42 GWh per year. The production capacity was kept the same as in the previous scenarios to maintain comparability. The capacity factors for wind energy are significantly higher and more stable throughout the year, when compared to solar energy (Fig. 3c). It was found that the required system power for the DBD system does not need to be 195 MW to obtain the total power of 508.42 GWh per year. As a result, the capacity of the wind farm is equal to the system power that the DBD system is designed for. This power was determined to be 94 MW, meaning both the capacity of the required wind farm is 94 MW, as well as the capacity of the DBD system. The largest Dutch onshore wind project called Windplan Groen went into operation in March 2024 and has an installed capacity of 515 MW, produced by 86 wind turbines.[59] Thus, the wind plant falls within the already realized range of wind farm sizes.

In order to produce the same amount of methanol, when using wind energy, a smaller DBD system is required. This results from there being less periods of low or no production when using wind energy. Furthermore, for solar energy the CF never exceeds 0.8 and there are a significant number of hours of no production. In contrast, for wind systems approximately 40% of the hours in a year have a CF of 1 and there are limited hours of low to no production, as shown in Fig. 5. Thus, the wind system can be seen as more efficient. However, in this case no surplus electricity is produced meaning there is no additional source of income from the selling of surplus electricity.

• Scenario #4

In scenario #4, constant electricity is supplied directly from the grid (prices relative to 2023). In this case there is no intermittency. Therefore, no storage capacity between the initial separation and the continuous separation is required, corresponding to the system shown in Fig. 2. The production capacity was kept the same as in the previous three scenarios, in order to maintain comparability. Therefore, the total power of 508.42 GWh per year was distributed over the full year of operation. In this case the operation was distributed over 8760 h, again to ensure consistency between all four scenarios. This resulted in a required input power for the DBD system of 58 MW.

• Scenario #5

To evaluate if the variable operation has a positive effect on the resulting MMSP, the process was simulated for constant

methanol production at 195 MW. In scenario #1 the surplus renewable energy used was priced at 0.002 € per kWh. For the constant production at 195 MW, additional electricity is taken from the grid when the amount of surplus renewable energy is not sufficient. The electricity from the grid is predicted to be fully renewable, at a cost of 0.012 € per kWh, in 2050.[56]

4. Cost assessment

The minimum selling price of methanol was calculated for scenarios #1–#4, at the two fractional methanol yields (Y = 0.11 and Y = 0.23). Furthermore, so far, multiple approaches have been developed for methanol production from direct CO_2 hydrogenation and their techno economic feasibility investigated. A MMSP of approximately 1000 € per t has been reported,[60–63] and this price was chosen as the benchmark and is indicated in Fig. 4a as a red line. In Fig. 4a it can be seen that scenario #4, which uses electricity from the grid and renewable H_2 for the year 2023, resulted in a significantly higher MMSP compared to the prospective scenarios #1–#3. This was expected as the variable operating costs are 25 to 45 times higher than the variable operating costs of the prospective scenarios, as shown in Fig. 4b. When comparing the three prospective scenarios, the one using surplus electricity (scenario #1) results in the lowest MMSP. However, it is evident that the plasma-assisted methanol production process cannot compete with other technologies producing methanol from CO_2 and H_2. Even at a high methanol yield, the MMSP for scenario #1 is 6717 € per t, which is more than 6 times higher than the benchmark.

From Fig. 4b it can be seen that for scenario #1 the fixed operating costs are the dominating factors. While the analysis for scenario #2 and scenario #3 shows that the annualized capital costs are the dominating cost factor, which is due to the contribution of the capital cost of the electricity systems. The high MMSP for scenario #2 among the prospective scenarios is attributable to the larger required capacity of the solar system compared to the wind system, which leads to significantly higher CAPEX for the energy system. The designed solar system produces excess solar energy, which is sold at 0.002 € per kWh and is accounted for as positive cash flow. However, this cannot compensate for the additional capital expenditures. In scenario #4 the dominating cost factor is the variable operating costs. Here prices for renewable H_2 and grid electricity prices in 2023 were used, which are significantly higher than the prospective prices for 2050. More specifically an electricity price of 0.26 € per kWh and H_2 price of 5.52 € per kg were employed.[64] The price of electricity has a strong influence on the costs of this process, due to the high energy consumption of plasma-assisted methanol production. Therefore, it can be seen that the use of surplus electricity in a prospective situation successfully reduced the variable operating costs and thereby the MMSP.

Furthermore, looking at the capital cost distribution depicted in Fig. 5, it emerges that in scenario #1 the cost of the plasma system (including reactors and power supply) makes up approximately 90% of the capital expenditure as shown in Fig. 5a, while the remaining 10% are the costs for the separation systems. The capital cost distribution for scenario #4 is similar to the one of scenario #1. On the other hand, for scenario #2 and scenario #3 the capital expenditures can be distributed into three aspects, namely the plasma system, the separation train and the electricity system. Approximately 71% and 63% of the capital expenditures account for the solar and wind system, respectively, as shown in Fig. 5b and c. Hence, significant additional capital was added for the off-grid systems, further clarifying why the resulting MMSP was higher for the off-grid scenarios, as compared to scenario #1. More details on the equipment costs are reported in Table S11 in the SI.

4.1 Comparison between variable and continuous operations

The ability to use surplus electricity and operate variably, based on electricity availability, is often seen as one of the main advantages of plasma systems. Therefore, in scenario #5, the process was simulated for a constant electricity supply to assess whether variable operation positively impacts the resulting MMSP. The resulting MMSP is shown in Fig. 6. For continuous production, additional electricity is drawn from the grid when surplus renewable energy is insufficient. This system is also assumed to operate 8760 hours per year, due to the use of the

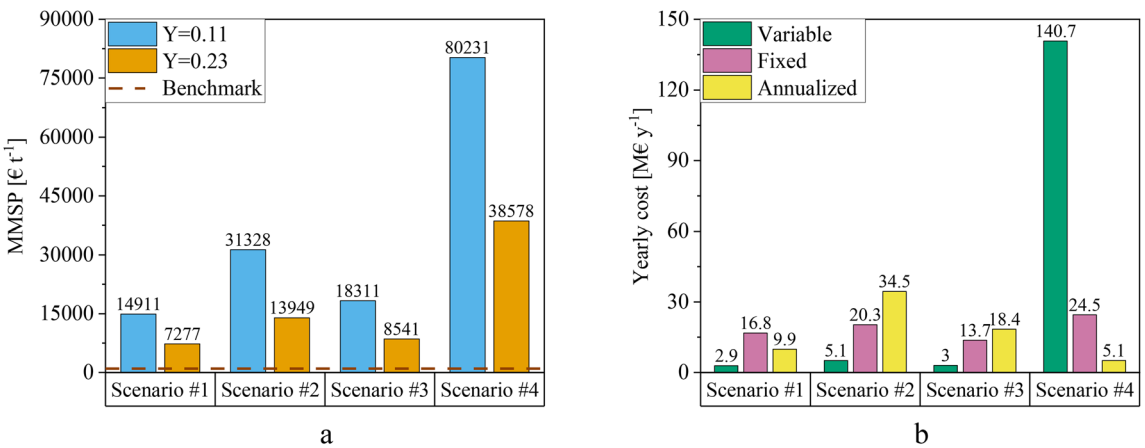

Fig. 4 (a) MMSP for the different scenarios and (b) annual costs comparison between scenarios #1–#4 investigated.

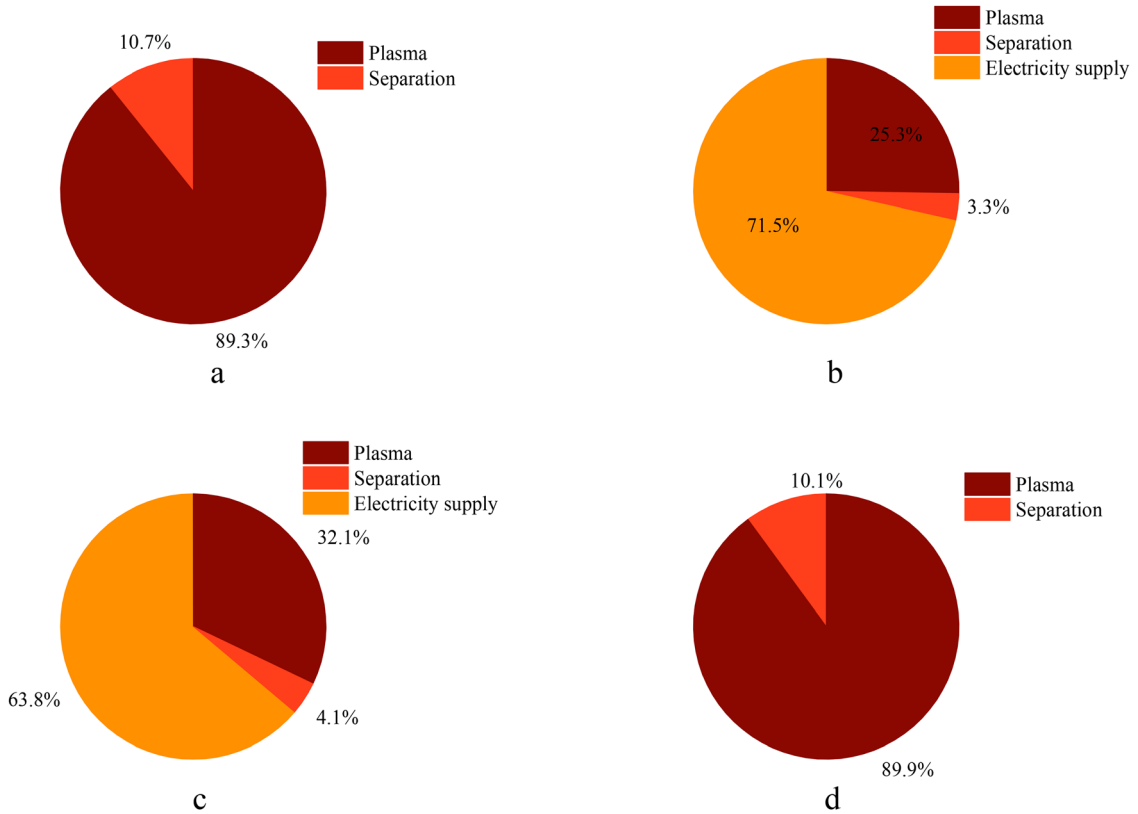

Fig. 5 Capital cost distribution between the plasma and separation systems for the fractional methanol yield Y = 0.11 for (a) scenario #1, (b) scenario #2, (c) scenario #3 and (d) scenario #4.

surplus electricity data and to maintain comparability between the investigated cases. Moving towards a constant methanol production, instead of a variable production, impacted several economic parameters. Firstly, the production of methanol increased from 2.14 kt per year to 7.21 kt per year, as the designed system was used at full capacity. This reflects the significant number of low or no production hours, in the case of using only surplus renewable energy. Secondly, the electricity cost for the plasma system increased, as more electricity was required and electricity needed to be purchased from the grid at a higher price. Finally, the operating costs of the continuous downstream separation system increased, as the reboiler duty and cooling water flow for the condensers increased, due to a larger flow of crude methanol that needed to be processed.

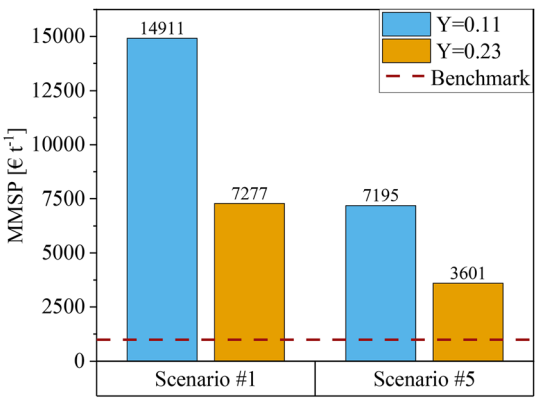

Fig. 6 Comparison of MMSP between the scenario of using surplus renewable energy and constant production at 195 MW, using both surplus renewable energy and grid electricity.

It can be seen that the MMSP is reduced to approximately half when using the plasma system constantly at its full capacity of 195 MW, for both methanol yield cases. Consequently, it can be concluded that the additional revenue provided by increasing the production of methanol is larger than the increased costs. These additional costs mainly include the higher electricity consumption of both the plasma system and the separation train, in combination with the higher price for electricity from the grid. This analysis demonstrates that due to the high capital expenditure and fixed costs of the process, the variable operation, in which the system is not used at its full capacity, is not favourable. Based on these findings, the advantage of the variably operating plasma system does not show the expected economic benefit for plasma-assisted methanol production, in the current situation.

4.2 Sensitivity analysis

Scenario #1 was chosen as the base case for sensitivity analyses as it resulted in the lowest MMSP, making it the most favourable scenario for potential optimization. Using this scenario as a reference allows for a fair comparison with future scenarios and provides insights into possible cost improvements. From the analysis of the main cost drivers, the following aspects were

chosen to be investigated in a one-factor sensitivity analysis: plasma CAPEX, total CAPEX, electricity price and H_2 price. The overall capital expenditure consists of the plasma system and the downstream separation of methanol. Due to the previously discussed strong contribution of the plasma CAPEX to the total CAPEX, these two aspects were investigated separately. In the sensitivity analysis, the aforementioned factors were varied between 0.5 and 1.5 times their original values, after which the corresponding MMSP was calculated. Of note, the sensitivity analysis in this study deliberately uses broad boundaries to reflect the significant uncertainty inherent in early-stage plasma-assisted CO_2 conversion technology. Because there is no commercial-scale plasma process for methanol production, reliable design data and cost estimates are lacking. The chosen ranges are based on the spread of reported lab-scale conversions, energy efficiencies, and CAPEX estimates in the literature, and are intended to capture best-case and worst-case scenarios rather than predict likely outcomes. Herein the independent effect of these factors on the economic performance of plasma-assisted methanol production could be determined, as shown in Fig. 7.

The total CAPEX has the most significant impact on the resulting MMSP, for both methanol yields. The net impact of the CAPEX reduction is lower in the case of high methanol yield, compared to the low methanol yield case. This can be attributed to the approximately doubled methanol production achieved without increasing the plasma system size while the total capital expenditures increased by only about 2%. This increase in capital expenditures is main due to the increase in complexity of downstream separation units required to handle higher methanol production rates. Finally, both the H_2 price and the electricity price have a comparably minimal effect on the MMSP. This is attributable to both the electricity and H_2 prices being prospective. The effect of the H_2 price is stronger for the case of higher yield, shown in Fig. 7b, due to the higher hydrogen consumption when more methanol is produced in the process. The results of the sensitivity analysis show that the benchmark price of 1000 € per t could not be reached by halving the contribution of the investigated factors.

It has to be mentioned that 50% power supply efficiency is assumed in our study, meaning 50% of the supplied power gets translated to plasma power.[43] Therefore, power supply systems might still have potential for further improvement. Fig. 8a shows that the MMSP decreases significantly as the power supply efficiency increases from 50 to 90%, for both methanol yields. The variation of the efficiency resulted in 21% and 20% decrease in MMSP for the yield of 0.11 and 0.23 respectively. Moreover, in Fig. 8b the MMSP as a function of the methanol yield is reported. A decrease in MMSP can be observed, caused by the reduced energy consumption with increasing yield. It can be seen that at no methanol yield the threshold price for methanol of 1000 € per t could be reached.

From those results, it is possible to conclude that focusing solely on a single factor does not show a feasible window for this process, meaning a possible combination of cost reductions is required to move closer to a competitive regime. For this reason, a two-factors sensitivity analysis has been conducted. The most influential factors, plasma CAPEX and the methanol yield, are considered. The CAPEX of plasma reactors is driven by several factors, including the cost of the power supply, electrode design, and reactor materials, all of which must be robust enough to operate under high-voltage conditions and resist reactive species. For plasma-based systems at the lab scale, the power supply unit is typically the most expensive component due to its flexibility to work with different plasma types, unlike power supplies for pilot or industrial scales, which can be optimized for specific operating conditions. For instance, Osorio-Tejada *et al.* estimated a cost of approximately 1085 € per kW (plasma power) for both the power unit and reactor body,[65] while O'Modhrain *et al.* reported the cost of the total reactor assembly, including the power supply, around 3000 € per kW, for a small scale of up to 1000 t per year.[66] Thus, prices reported in the literature for plasma reactor systems are highly variable, further underscoring the

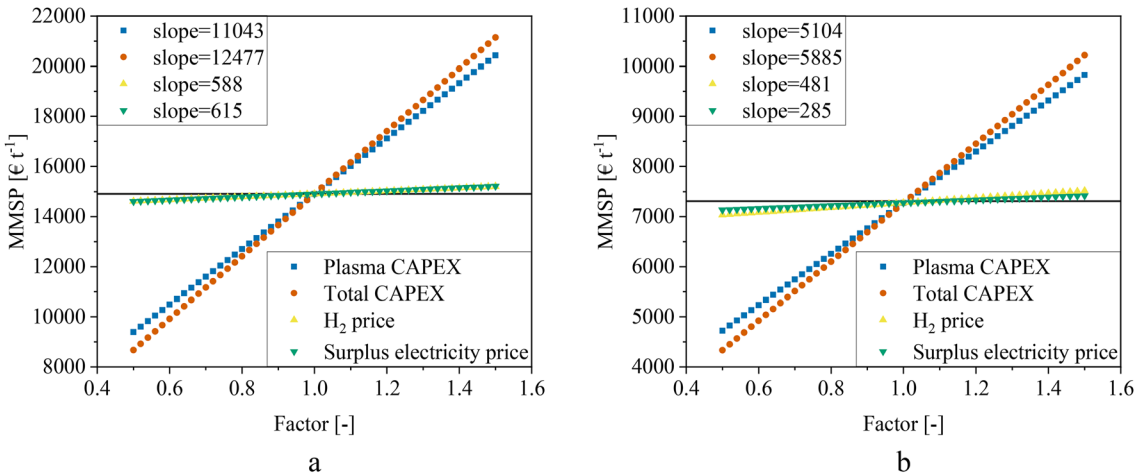

Fig. 7 One-factor sensitivity analysis showing the effect of increasing and decreasing plasma CAPEX, total fixed cost, H_2 price, and surplus electricity price between 0.5 and 1.5 times the original value for the two fractional methanol yields (a) Y = 0.11 and (b) Y = 0.23.

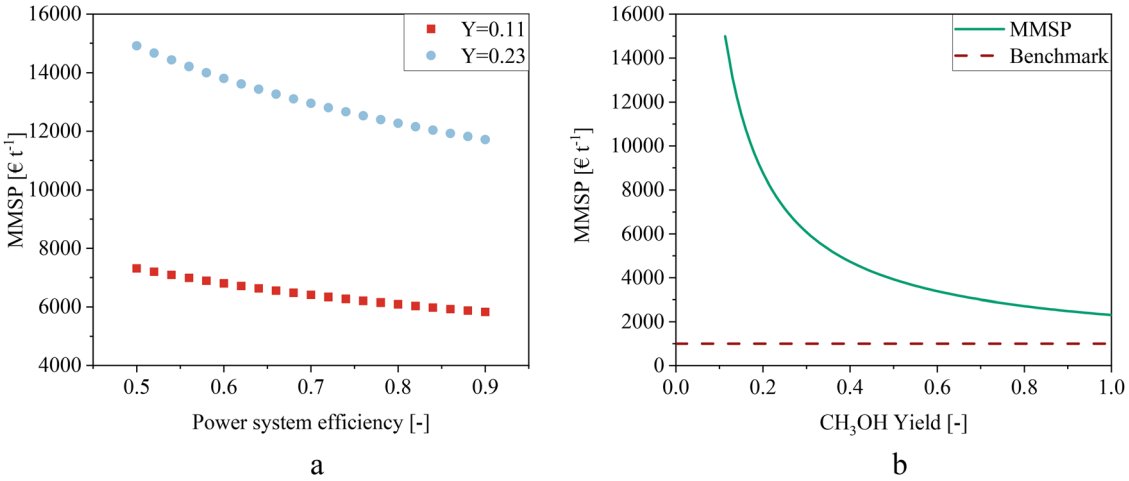

Fig. 8 Effect of (a) power supply efficiency on the resulting MMSP for the two fractional methanol yields Y = 0.11 and Y = 0.23 and (b) increasing yield on the MMSP.

need for careful sensitivity analysis to account for this uncertainty. These considerations underscore the potential for significant cost reduction through scale-up, modular design, and targeted improvements in power supply efficiency and durable electrode materials. We also note that although more recent cost data are available for GAP-type reactors, these could not be used here because they pertain to a different plasma configuration (GAP) rather than the dielectric barrier discharge (DBD) systems considered in this study. The combined effect on the plasma system was simulated. The resulting MMSP was calculated in five different cases of reduced plasma system CAPEX, namely 100%, 50%, 20%, 10%, and 1% of the original CAPEX of the plasma system. In Fig. 9, it can be seen that the benchmark price of 1000 € per t for methanol cannot be reached under the investigated conditions.

It is important to note that when the plasma CAPEX is decreased significantly the other costs, such as separation CAPEX, the raw material costs and the electricity costs become more relevant. Fig. 10 presents a one-factor-at-a-time sensitivity analysis conducted at different plasma CAPEX levels to evaluate the influence of key cost factors. Specifically, the analysis explores the effects of total CAPEX, H_2 price, and surplus electricity price on the variation of the MMSP. The results reveal that at high plasma CAPEX, its impact on the total CAPEX is more substantial, making it the dominant factor in determining overall project costs. Conversely, when plasma CAPEX is significantly reduced, the costs of surplus electricity and hydrogen gain greater relevance, suggesting that these factors could become the primary drivers of economic viability under lower plasma CAPEX scenarios.

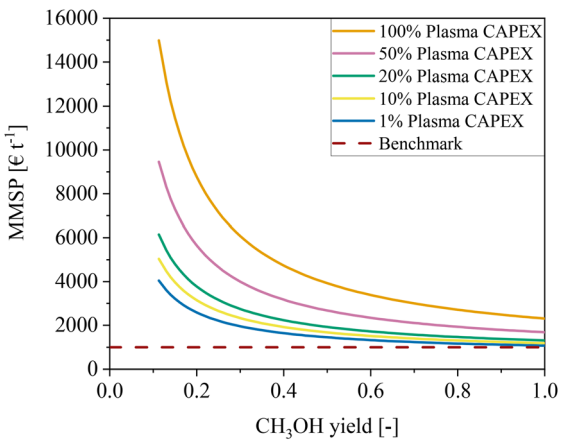

Fig. 9 Effect of methanol yield and reducing capital cost of the plasma system on the MMSP for scenario #1.

The implementation of constant methanol production at 195 MW input power into the plasma system, shown in Fig. 6, reduced the MMSP significantly, however the benchmark was not reached. The MMSP was reduced to 3601 € per t at Y = 0.23. Even though the MMSP is lower than for variable operation, it is still significantly above the benchmark of 1000 € per t. Subsequently, an analysis of the effect of reduced plasma CAPEX and increased methanol yield was conducted on this configuration. Fig. 11 shows that when operating the plasma-assisted methanol plant constantly, the benchmark price can be reached at 20% of the plasma CAPEX and a methanol yield of 0.87.

To improve the economic viability of plasma-assisted CO_2 conversion to methanol, it is essential to target higher conversion rates and energy efficiencies through advances in catalyst development and reactor design. A key factor to improving process efficiency in NTP systems is the rational design of catalysts tailored for plasma environments. Recent work on siliceous mesocellular foam (MCF) supported Cu catalysts for NTP-catalytic CO_2 hydrogenation to methanol demonstrated that the MCF support, with its high specific surface area (784 $m^2\ g^{-1}$) and large mesopores ($\sim$8.5 nm), enhances plasma discharge characteristics and facilitates species diffusion, outperforming other porous materials.[67] Furthermore, reactor design improvements, including optimized electrode configurations, power modulation strategies, and better thermal

management, have been demonstrated to significantly increase energy efficiency. For example, recent study investigated the impact of high-voltage electrode configuration and materials (Cu, Al, stainless steel SUS304) in a temperature-controlled

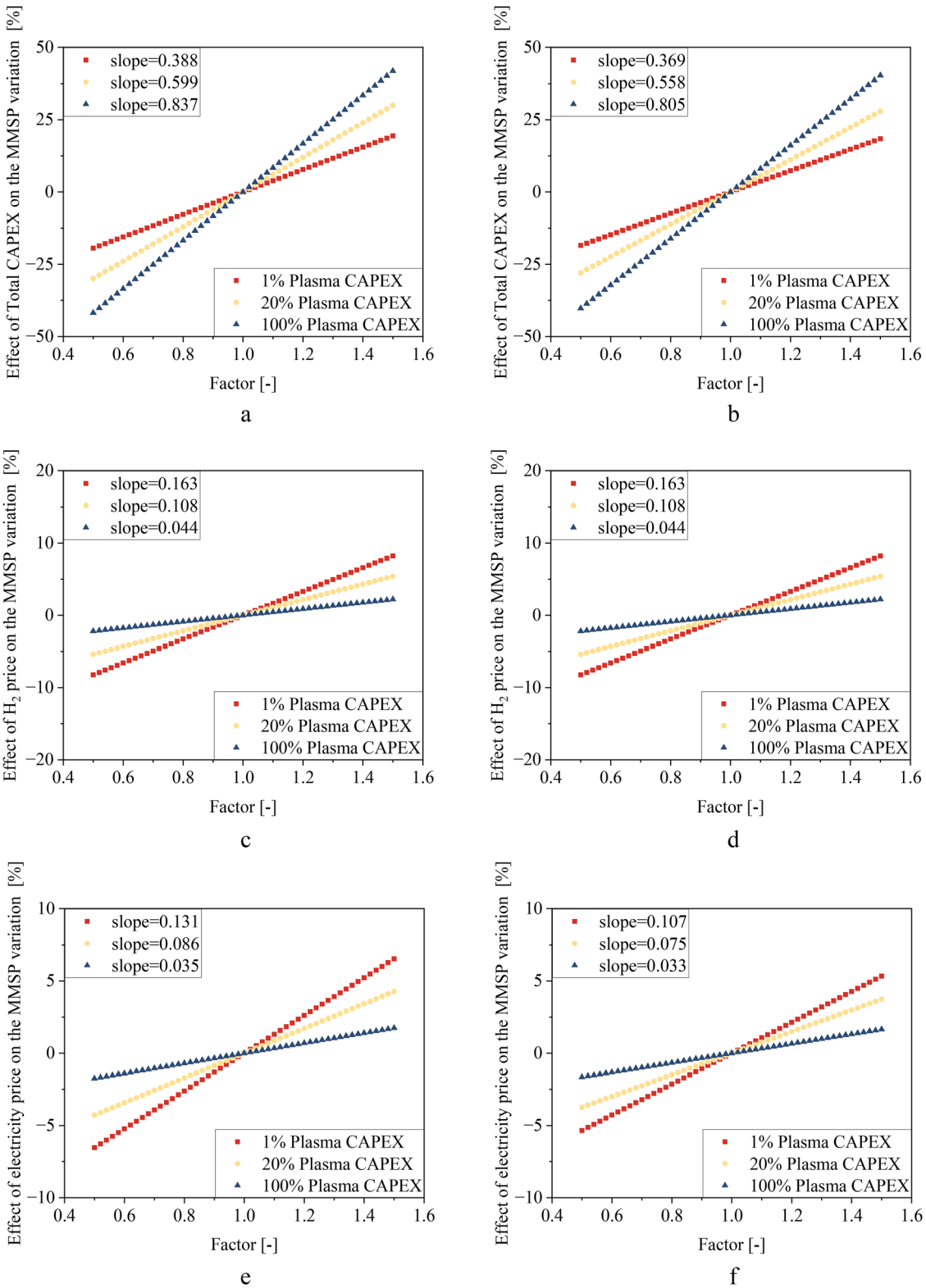

Fig. 10 One-factor sensitivity analysis, at different plasma CAPEX. Showing the effect of increasing and decreasing total CAPEX at the fractional methanol yields (a) $Y = 0.11$ and (b) $Y = 0.23$, H_2 price at (c) $Y = 0.11$ and (d) $Y = 0.23$, and surplus electricity price at (e) $Y = 0.11$ and (f) $Y = 0.23$ between 0.5 and 1.5 times the original value.

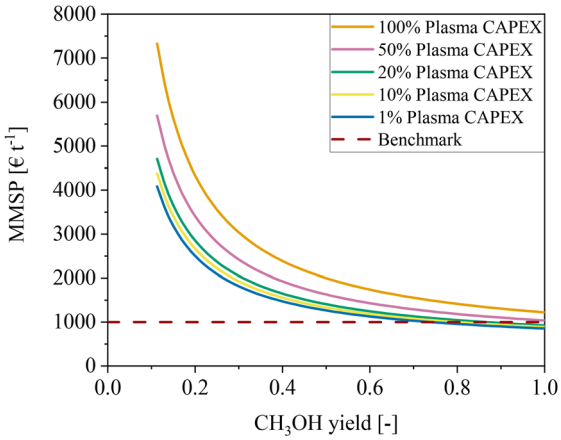

Fig. 11 Effect of methanol yield and reduced CAPEX of the plasma system on the MMSP when the production is constant at 195 MW, using both surplus and grid electricity.

pulsed DBD reactor, showing that Cu electrodes delivered superior methanol production (0.14 mmol kWh^{-1}) due to their catalytic activity, while Al electrodes performed worst (0.08 mmol kWh^{-1}) because of surface oxide passivation.[68] Another study explored the non-catalytic hydrogenation of CO_2 and CO gas mixtures in a self-cooling DBD plasma at atmospheric pressure and temperature, using small amounts of N_2 and argon as auxiliary gases to influence methanol production.[69] N_2 reduced plasma power requirements, stabilized the discharge, and acted as a beneficial third body to tune plasma reactions, yielding better methanol production rates than argon. These findings demonstrate that plasma performance can be significantly enhanced by optimizing reactant compositions and gas additives, providing a promising strategy to improve methanol synthesis.

5. Uncertainty analysis

In a techno-economic analysis typically 8000 operating hours per year are assumed.[55,70] However, throughout the scenario analysis in this work an operating year of 8760 hours was considered. This was done, as data on the surplus renewable energy and the capacity factors for the off-grid systems were available for the full year. It was deemed unreasonable to arbitrarily remove 760 hours from any time of the year, as this requires a more thorough analysis to identify the optimal period for production downtime. This was seen to be outside the scope of this work. Not accounting for downtime may overestimate system efficiency and resource utilization, particularly since the process involves a catalyst, making deactivation, regeneration, and maintenance crucial. However, since this assumption was consistently applied across all scenarios, the comparability of conclusions remains unaffected. Nevertheless, this aspect should be considered when comparing the results to other processes, where scheduled downtime may impact overall performance and feasibility.

During the scale-up of the plasma reactors, it was assumed that the CO_2 conversion and the product selectivities remain the same as experimental results. These assumptions were based on previously conducted techno economic studies and supported by few experimental studies.[38,46] However, there are limited studies which demonstrate how the large increase in reactor dimensions could influence on its performance, particularly in a packed-bed DBD reactor with catalysts. In order to eliminate these uncertainties, pilot scale studies with sized up DBD reactors are needed.

Within scenario #1–#3, the economic analysis was made using a prospective approach. This was done for the H_2 price in all three scenarios, for the electricity price in scenario #1 and the off-grid electricity systems in scenario #2 and #3. Besides these points, the cost factors, such as separation equipment, catalysts, and labour, were not adjusted due to a lack of projections for 2050, though the plasma system's capital cost was separately analyzed for potential reductions. Furthermore, the three prospective scenarios are based on the study on the power system of the Netherlands in 2050. Within this study it was noted that the COMPETES model predicts a relatively high supply of renewable energy, in combination with a relatively low electricity demand. This could lead to an overestimation of surplus energy availability and low electricity prices, particularly affecting scenario #1, where production relies solely on surplus electricity. If the renewable electricity supply is lower and the demand is higher than predicted, this could also increase the grid electricity price in 2050, above the predicted 0.012 € per kWh. A higher-than-expected grid electricity price could impact the comparative economics of variable *versus* constant methanol production.

6. Conclusions

In this study, the effects of multiple energy supply strategies on the competitiveness of plasma-assisted methanol production were investigated. The results show that in all the range of investigated scenarios the MMSP was higher than the benchmark. Scenario #4, set in 2023, resulted in a MMSP 30–80 times higher due to the high variable operating costs. This demonstrated the need for low priced electricity for this process to compensate the high energy consumption. Subsequently, the three prospective scenarios in 2050 were investigated, for which the MMSP reduced significantly. Scenario #1, in which surplus renewable energy was used, resulted in the lowest MMSP. However, the MMSP was still more than seven times higher than the benchmark price. A comparison between a variable system and a system operating continuously at maximum capacity revealed significantly better economic performance for the continuous system. The MMSP was approximately halved compared to that of the variable system. Thus, while plasma technologies allow for variable operation, this flexibility did not deliver the anticipated economic benefits for plasma-assisted methanol production from CO_2 and H_2 at the current stage.

The economic feasibility of plasma-assisted methanol production is shown to be highly sensitive to electricity prices. Given the high energy demands of plasma processes, securing

affordable and reliable electricity sources is essential for this method to be economically viable. However, even under ideal conditions, where surplus electricity is available at a low cost and other operational expenses are minimized, plasma-assisted methods still struggle to compete with more conventional thermocatalytic CO_2 hydrogenation processes. The study therefore emphasizes that further technological advancements are necessary to reach competitive levels. In particular, innovations in plasma power supply systems are needed to enhance energy efficiency and cut down the substantial costs that currently hinder the process.

Conflicts of interest

The authors declare that they have no known competing interests that could have appeared to influence the work in this paper.

Abbreviations

CAPEX	Capital expenditure
CCU	Carbon capture and utilization
CEPCI	Chemical engineering plant cost index
CF	Capacity factor
COMPETES	Competition and market power in electric transmission and energy simulator
DBD	Dielectric barrier discharge
DS	Design specification
DW&B	Direct wages and benefits
FCI	Fixed capital investment
HV	High voltage
HX	Heat exchanger
IRENA	International renewable energy agency
M&O-S&B	Maintenance and operations-salary, wages and benefits
MMSP	Minimum methanol selling price
MW&B	Maintenance wages and benefits
NPV	Net present value
NRTL-RK	Non-random two-liquid-Redlich–Kwong
NTP	Non-thermal plasma
OPEX	Operating expenditure
PFD	Process flow diagram
ppm	Parts per million
REFPROP	Reference fluid thermodynamic and transport properties
TNO	Netherlands organization for applied scientific research

Data availability

Supplementary information is available. This supplementary information includes detailed stream tables and additional data relevant to the cost assessment. See DOI: **https://doi.org/10.1039/d5ey00130g**

The data supporting this article have been included as part of the manuscript and the SI.

Acknowledgements

The authors gratefully acknowledge Jos Sijm for providing the data on the curtailed electricity and capacity factor in the Netherlands used in this study.

References

1 Renewable Energy Highlights Electricity Generation by Energy Source Fossil Fuels Nuclear Other Non-Renewables Pumped Storage Renewables % Renewables % Variable Renewables; 2024.
2 CO2 Emissions in 2022. *CO2 Emissions in 2022*, 2023, DOI: **10.1787/12ad1e1a-en**.
3 D. A. R. Barkhouse, O. Gunawan, T. Gokmen, T. K. Todorov and D. B. Mitzi, Yield Predictions for Photovoltaic Power Plants:Empirical Validation, Recent Advances and Remaining Uncertainties, *Prog. Photovoltaics Res. Appl.*, 2015, **20**, 6–11, DOI: **10.1002/pip**.
4 C. S. Lai, G. Locatelli, A. Pimm, X. Wu and L. L. Lai, A Review on Long-Term Electrical Power System Modeling with Energy Storage, *J. Cleaner Prod.*, 2021, **280**, 124298, DOI: **10.1016/j.jclepro.2020.124298**.
5 A. G. Olabi, C. Onumaegbu, T. Wilberforce, M. Ramadan, M. A. Abdelkareem and A. H. Al-Alami, Critical Review of Energy Storage Systems, *Energy*, 2021, **214**, 118987, DOI: **10.1016/J.ENERGY.2020.118987**.
6 A. Varone and M. Ferrari, Power to Liquid and Power to Gas: An Option for the German Energiewende, *Renewable Sustainable Energy Rev.*, 2015, **45**, 207–218, DOI: **10.1016/j.rser.2015.01.049**.
7 B. R. de Vasconcelos and J. M. Lavoie, Recent Advances in Power-to-X Technology for the Production of Fuels and Chemicals, *Front. Chem.*, 2019, **7**, 1–24, DOI: **10.3389/fchem.2019.00392**.
8 V. Battaglia and L. Vanoli, Optimizing Renewable Energy Integration in New Districts: Power-to-X Strategies for Improved Efficiency and Sustainability, *Energy*, 2024, **305**, 132312, DOI: **10.1016/J.ENERGY.2024.132312**.
9 J. Martin-Del-Campo, S. Coulombe and J. Kopyscinski, Influence of Operating Parameters on Plasma-Assisted Dry Reforming of Methane in a Rotating Gliding Arc Reactor, *Plasma Chem. Plasma Process.*, 2020, **40**, 857–881, DOI: **10.1007/s11090-020-10074-2**.
10 S. Saeidi, N. A. S. Amin and M. R. Rahimpour, Hydrogenation of CO2 to Value-Added Products – A Review and Potential Future Developments, *J. CO2 Util.*, 2014, **5**, 66–81, DOI: **10.1016/j.jcou.2013.12.005**.
11 M. Pérez-Fortes, J. C. Schöneberger, A. Boulamanti and E. Tzimas, Methanol Synthesis Using Captured CO2 as Raw Material: Techno-Economic and Environmental Assessment, *Appl. Energy*, 2016, **161**, 718–732, DOI: **10.1016/j.apenergy.2015.07.067**.
12 M. Q. Feliz, I. Polaert, A. Ledoux, C. Fernandez and F. Azzolina-Jury, Influence of Ionic Conductivity and Dielectric Constant of the Catalyst on DBD Plasma-Assisted

CO2hydrogenation into Methanol, *J. Phys. D: Appl. Phys.*, 2021, **54**, 334003, DOI: 10.1088/1361-6463/abfddd.
13 M. D. Farahani, Y. Zeng and Y. Zheng, The Application of Nonthermal Plasma in Methanol Synthesis via CO2 Hydrogenation, *Energy Sci. Eng.*, 2022, **10**, 1572–1583.
14 M. Scomazzon, E. Barbera and F. Bezzo, Alternative Sustainable Routes to Methanol Production: Techno-Economic and Environmental Assessment, *J. Environ. Chem. Eng.*, 2024, **12**(3), 112674, DOI: 10.1016/j.jece.2024.112674.
15 D. Mei, X. Zhu, C. Wu, B. Ashford, P. T. Williams and X. Tu, Plasma-Photocatalytic Conversion of CO2 at Low Temperatures: Understanding the Synergistic Effect of Plasma-Catalysis, *Appl. Catal., B*, 2016, **182**, 525–532, DOI: 10.1016/j.apcatb.2015.09.052.
16 Y. L. Men, Y. Liu, Q. Wang, Z. H. Luo, S. Shao, Y. B. Li and Y. X. Pan, Highly Dispersed Pt-Based Catalysts for Selective CO2 Hydrogenation to Methanol at Atmospheric Pressure, *Chem. Eng. Sci.*, 2019, **200**, 167–175, DOI: 10.1016/j.ces.2019.02.004.
17 R. K. Masumbuko, N. Kobayashi, Y. Itaya and A. Suami, Enhanced Methanol Selectivity and Synthesis in a Non-Catalytic Dielectric Barrier Discharge (DBD) Plasma Reactor, *Chem. Eng. Sci.*, 2024, **287**, 119698, DOI: 10.1016/J.CES.2023.119698.
18 Z. Cui, S. Meng, Y. Yi, A. Jafarzadeh, S. Li, E. C. Neyts, Y. Hao, L. Li, X. Zhang and X. Wang, Plasma-Catalytic Methanol Synthesis from CO_2 Hydrogenation over a Supported Cu Cluster Catalyst: Insights into the Reaction Mechanism, *ACS Catal.*, 2022, **12**(2), DOI: 10.1021/acscatal.1c04678.
19 L. Wang, Y. Yi, H. Guo and X. Tu, Atmospheric Pressure and Room Temperature Synthesis of Methanol through Plasma-Catalytic Hydrogenation of CO2, *ACS Catal.*, 2018, **8**, 90–100, DOI: 10.1021/acscatal.7b02733.
20 Y. L. Men, Y. Liu, Q. Wang, Z. H. Luo, S. Shao, Y. B. Li and Y. X. Pan, Highly Dispersed Pt-Based Catalysts for Selective CO2 Hydrogenation to Methanol at Atmospheric Pressure, *Chem. Eng. Sci.*, 2019, **200**, 167–175, DOI: 10.1016/J.CES.2019.02.004.
21 N. Joshi and S. Loganathan, Methanol Synthesis from CO2 Using Ni and Cu Supported Fe Catalytic System: Understanding the Role of Nonthermal Plasma Surface Discharge, *Plasma Processes Polym.*, 2021, **18**(5), DOI: 10.1002/ppap.202000104.
22 Q. Chen, S. Meng, R. Liu, X. Zhai, X. Wang, L. Wang, H. Guo and Y. Yi, Plasma-Catalytic CO2 Hydrogenation to Methanol over CuO-MgO/Beta Catalyst with High Selectivity, *Appl. Catal., B*, 2024, **342**, 123422, DOI: 10.1016/j.apcatb.2023.123422.
23 S. Meng, L. Wu, M. Liu, Z. Cui, Q. Chen, S. Li, J. Yan, L. Wang, X. Wang and J. Qian, *et al.*, Plasma-Driven CO2 Hydrogenation to CH3OH over Fe2O3/γ-Al2O3 Catalyst, *AIChE J.*, 2023, **69**, 1–14, DOI: 10.1002/aic.18154.
24 S. Li, G. De Felice, S. Eichkorn, T. Shao and F. Gallucci, A Review on Plasma-Based CO2 Utilization: Process Considerations in the Development of Sustainable Chemical Production, *Plasma Sci. Technol.*, 2024, **26**, 094001, DOI: 10.1088/2058-6272/ad52c4.
25 N. Joshi and S. Loganathan, Methanol Synthesis from CO2 Using Ni and Cu Supported Fe Catalytic System: Understanding the Role of Nonthermal Plasma Surface Discharge, *Plasma Processes Polym.*, 2021, **18**(5), DOI: 10.1002/ppap.202000104.
26 U. Kogelschatz, Dielectric-Barrier Discharges: Their History, Discharge Physics, and Industrial Applications, *Plasma Chem. Plasma Process.*, 2003, **23**, 1–46.
27 S. J. Kaufmann, P. Rößner, S. Renninger, M. Lambarth, M. Raab, J. Stein, V. Seithümmer and K. P. Birke, Techno-Economic Potential of Plasma-Based CO_2 Splitting in Power-to-Liquid Plants, *Appl. Sci.*, 2023, **13**, 4839, DOI: 10.3390/app13084839.
28 G. Manzolini, A. Giuffrida, P. D. Cobden, H. A. J. van Dijk, F. Ruggeri and F. Consonni, Techno-Economic Assessment of SEWGS Technology When Applied to Integrated Steel-Plant for CO2 Emission Mitigation, *Int. J. Greenhouse Gas Control*, 2020, **94**, 102935, DOI: 10.1016/j.ijggc.2019.102935.
29 J. Burgess, *Netherlands Begins Construction of National Hydrogen Pipeline Network*, S&P Global, 2023, pp. 0–3.
30 É. S. Van-Dal and C. Bouallou, Design and Simulation of a Methanol Production Plant from CO2 Hydrogenation, *J. Cleaner Prod.*, 2013, **57**, 38–45, DOI: 10.1016/j.jclepro.2013.06.008.
31 A. A. Kiss, J. J. Pragt, H. J. Vos, G. Bargeman and M. T. de Groot, Novel Efficient Process for Methanol Synthesis by CO2 Hydrogenation, *Chem. Eng. J.*, 2016, **284**, 260–269, DOI: 10.1016/j.cej.2015.08.101.
32 C. Carlson, *Eric Succeed in G At Sim U Lation*, 1996, pp. 35–46.
33 M. L. Huber, E. W. Lemmon, I. H. Bell and M. O. McLinden, The NIST REFPROP Database for Highly Accurate Properties of Industrially Important Fluids, *Ind. Eng. Chem. Res.*, 2022, **61**, 15449–15472, DOI: 10.1021/acs.iecr.2c01427.
34 R. Brandenburg, Dielectric Barrier Discharges: Progress on Plasma Sources and on the Understanding of Regimes and Single Filaments, *Plasma Sources Sci. Technol.*, 2018, **27**(5), DOI: 10.1088/1361-6595/aaced9.
35 G. Vezzu, J. L. Lopez, A. Freilich and K. H. Becker, Optimization of Large-Scale Ozone Generators, *IEEE Trans. Plasma Sci.*, 2009, **37**, 890–896, DOI: 10.1109/TPS.2009.2015452.
36 U. Kogelschatz, Dielectric-Barrier Discharges: Their History, Discharge Physics, and Industrial Applications, *Plasma Chem. Plasma Process.*, 2003, **23**, 1–46.
37 H. Yamasaki, Y. Mizuguchi, R. Nishioka, Y. Fukuda, T. Kuroki, H. Yamamoto and M. Okubo, Pilot-Scale NOx and SOx Aftertreatment by Semi-Dry Plasma-Chemical Hybrid Process in Glass-Melting-Furnace Exhaust Gas, *Plasma Chem. Plasma Process.*, 2022, **42**, 51–71, DOI: 10.1007/s11090-021-10193-4.
38 A. A. Assadi, A. Bouzaza and D. Wolbert, Comparative Study between Laboratory and Large Pilot Scales for VOC's Removal from Gas Streams in Continuous Flow Surface Discharge Plasma, *Chem. Eng. Res. Des.*, 2016, **106**, 308–314, DOI: 10.1016/j.cherd.2015.12.025.
39 R. K. Masumbuko, N. Kobayashi, Y. Itaya and A. Suami, Enhanced Methanol Selectivity and Synthesis in a Non-

Catalytic Dielectric Barrier Discharge (DBD) Plasma Reactor, *Chem. Eng. Sci.*, 2024, **287**, 119698, DOI: **10.1016/J.CES.2023.119698**.

40 M. Umamaheswara Rao, K. V. S. S. Bhargavi, P. Chawdhury, D. Ray, S. R. K. Vanjari and C. Subrahmanyam, Non-Thermal Plasma Assisted CO2 Conversion to CO: Influence of Non-Catalytic Glass Packing Materials, *Chem. Eng. Sci.*, 2023, **267**, 118376, DOI: **10.1016/J.CES.2022.118376**.

41 V. Spallina, I. C. Velarde, J. A. M. Jimenez, H. R. Godini, F. Gallucci and M. Van Sint Annaland, Techno-Economic Assessment of Different Routes for Olefins Production through the Oxidative Coupling of Methane (OCM): Advances in Benchmark Technologies, *Energy Convers. Manage.*, 2017, **154**, 244–261, DOI: **10.1016/j.enconman.2017.10.061**.

42 W. D. Seider, D. R. Lewin, J. D. Seader, S. Widagdo, R. Gani and K. M. Ng, *Product and Process Design Principles: Synthesis, Analysis, and Evaluation*, John Wiley & Sons, 2017, ISBN 1119282632.

43 J. Cran, Cost Indices, *Eng. Process Econ.*, 1976, **1**, 13–23, DOI: **10.1016/0377-841X(76)90042-5**.

44 R. Davis, H. Olcay, M. Talmadge, J. Dempsey, L. Tao, B. Klein, E. C. D. Tan, T. N. Do, L. Ou and H. Cai, Technology Case Study: Economic, Sustainability, and Deployment Considerations for Sustainable Aviation Fuels Produced via Lignocellulosic Sugar Catalysis, 2025, DOI: **10.2172/2522760**.

45 Bureau of Labor Statistics Available online: **https://data.bls.gov/pdq/SurveyOutputServlet** (accessed on 4 July 2025).

46 H. Lamberts-Van Assche, G. Thomassen and T. Compernolle, The Early-Stage Design of Plasma for the Conversion of CO2to Chemicals: A Prospective Techno-Economic Assessment, *J. CO2 Util.*, 2022, **64**, 102156, DOI: **10.1016/j.jcou.2022.102156**.

47 G. J. Van Rooij, H. N. Akse, W. A. Bongers and M. C. M. Van De Sanden, Plasma for Electrification of Chemical Industry: A Case Study on CO2 Reduction, *Plasma Phys. Controlled Fusion*, 2018, **60**, 014019, DOI: **10.1088/1361-6587/aa8f7d**.

48 F. G. Baddour, L. Snowden-Swan, J. D. Super and K. M. Van Allsburg, Estimating Precommercial Heterogeneous Catalyst Price: A Simple Step-Based Method, *Org. Process Res. Dev.*, 2018, **22**, 1599–1605, DOI: **10.1021/acs.oprd.8b00245**.

49 L. Sens, U. Neuling and M. Kaltschmitt, Capital Expenditure and Levelized Cost of Electricity of Photovoltaic Plants and Wind Turbines – Development by 2050, *Renewable Energy*, 2022, **185**, 525–537, DOI: **10.1016/j.renene.2021.12.042**.

50 C. P. Operator; E. Our and S. Database, *Most Popular Skills for Chemical Plant Operator Job Description*, 2024, pp. 24–27.

51 S. Michailos, S. McCord, V. Sick, G. Stokes and P. Styring, Dimethyl Ether Synthesis via Captured CO2 Hydrogenation within the Power to Liquids Concept: A Techno-Economic Assessment, *Energy Convers. Manage.*, 2019, **184**, 262–276, DOI: **10.1016/J.ENCONMAN.2019.01.046**.

52 De Nederandsche Bank. Interest Rates, 2024.

53 CEIC DATA. Netherlands Long Term Interest Rate, 2024. Available online: **https://www.ceicdata.com/en/indicator/netherlands/long-term-interest-rate** (accessed on 26 July 2024).

54 A. A. Kiss, J. J. Pragt, H. J. Vos, G. Bargeman and M. T. de Groot, Novel Efficient Process for Methanol Synthesis by CO2 Hydrogenation, *Chem. Eng. J.*, 2016, **284**, 260–269, DOI: **10.1016/j.cej.2015.08.101**.

55 S. Poto, T. Vink, P. Oliver, F. Gallucci and M. F. Neira D'angelo, Techno-Economic Assessment of the One-Step CO2conversion to Dimethyl Ether in a Membrane-Assisted Process, *J. CO2 Util.*, 2023, **69**, 102419, DOI: **10.1016/j.jcou.2023.102419**.

56 J. Sijm, G. Morale-España and R. Hernández-Serna, *The Role of Demand Response in the Power System of the Netherlands*. *Tno*, 2022, pp. 1–155.

57 T. Gill The 15 Largest Solar Farms in the World 2024. The eco experts 2024, pp. 1–20.

58 S. Enkhardt, Europe's Largest PV Plant Goes Online. PV magazine 2024, pp. 2–7.

59 P. Griffiths, *More Projects*. *The Economist's Tale*, 2021, pp. 1–5, DOI: **10.5040/9781350250987.0023**.

60 S. Sollai, A. Porcu, V. Tola, F. Ferrara and A. Pettinau, Renewable Methanol Production from Green Hydrogen and Captured CO2: A Techno-Economic Assessment, *J. CO2 Util.*, 2023, **68**, 102345, DOI: **10.1016/j.jcou.2022.102345**.

61 J. Kim, C. A. Henao, T. A. Johnson, D. E. Dedrick, J. E. Miller, E. B. Stechel and C. T. Maravelias, Methanol Production from CO_2 Using Solar-Thermal Energy: Process Development and Techno-Economic Analysis, *Energy Environ. Sci.*, 2011, **4**, 3122–3132, DOI: **10.1039/c1ee01311d**.

62 H. Nieminen, A. Laari and T. Koiranen, CO2 Hydrogenation to Methanol by a Liquid-Phase Process with Alcoholic Solvents: A Techno-Economic Analysis, *Processes*, 2019, **7**, 1–24, DOI: **10.3390/pr7070405**.

63 S. Szima and C. C. Cormos, Improving Methanol Synthesis from Carbon-Free H2 and Captured CO2: A Techno-Economic and Environmental Evaluation, *J. CO2 Util.*, 2018, **24**, 555–563, DOI: **10.1016/j.jcou.2018.02.007**.

64 R. J. Detz, J. N. H. Reek and B. C. C. Van Der Zwaan, The Future of Solar Fuels: When Could They Become Competitive?, *Energy Environ. Sci.*, 2018, **11**, 1653–1669, DOI: **10.1039/c8ee00111a**.

65 J. Osorio-Tejada, M. Escriba-Gelonch, R. Vertongen, A. Bogaerts and V. Hessel, CO2 Conversion to CO via Plasma and Electrolysis: A Techno-Economic and Energy Cost Analysis, *Energy Environ. Sci.*, 2024, **17**, 5833–5853, DOI: **10.1039/d4ee00164h**.

66 C. O'Modhrain, G. Trenchev, Y. Gorbanev and A. Bogaerts, Upscaling Plasma-Based CO 2 Conversion: Case Study of a Multi-Reactor Gliding Arc Plasmatron, *ACS Eng. Au*, 2024, **4**, 333–344, DOI: **10.1021/acsengineeringau.3c00067**.

67 Y. Chen, S. Chen, Y. Shao, C. Quan, N. Gao, X. Fan and H. Chen, Siliceous Mesocellular Foam Supported Cu Catalysts for Promoting Non-Thermal Plasma Activated CO2 Hydrogenation toward Methanol Synthesis, *Front. Chem. Sci. Eng.*, 2024, **18**(77), DOI: **10.1007/s11705-024-2419-z**.

68 R. K. Masumbuko, N. Kobayashi, A. Suami, Y. Itaya and B. Zhang, Effect of High Voltage Electrode Material on Methanol Synthesis in a Pulsed Dielectric Barrier Discharge Plasma Reactor, *Catalysts*, 2024, **14**(12), 891, DOI: **10.3390/catal14120891**.

69 R. K. Masumbuko, N. Kobayashi, Y. Itaya and A. Suami, Enhanced Methanol Selectivity and Synthesis in a Non-Catalytic Dielectric Barrier Discharge (DBD) Plasma Reactor, *Chem. Eng. Sci.*, 2024, **287**, 119698, DOI: **10.1016/J.CES.2023.119698**.

70 M. Pérez-Fortes, J. C. Schöneberger, A. Boulamanti and E. Tzimas, Methanol Synthesis Using Captured CO2 as Raw Material: Techno-Economic and Environmental Assessment, *Appl. Energy*, 2016, **161**, 718–732, DOI: **10.1016/j.apenergy.2015.07.067**.